Published in final edited form as:

Mol Cancer Res. 2022 March 01; 20(3): 350–360. doi:10.1158/1541-7786.MCR-21-0536.

Epigenetic Silencing of 15-Hydroxyprostaglandin Dehydrogenase by Histone Methyltransferase EHMT2/G9a in Cholangiocarcinoma

Jinqiang Zhang, **Weina Chen**, **Wenbo Ma**, **Kyoungsub Song**, **Sean Lee**, **Chang Han**, **Tong Wu**

Department of Pathology and Laboratory Medicine, Tulane University School of Medicine, New Orleans, LA 70112

Abstract

Cholangiocarcinoma (CCA) is a lethal malignancy with few therapeutic options. NAD+-dependent 15-hydroxyprostaglandin dehydrogenase (15-PGDH) has been shown to inhibit CCA cell growth in vitro and in xenograft models. However, the role of 15-PGDH in CCA development has not been investigated and the mechanism for 15-PGDH gene regulation remains unclear. Here, we evaluated the role of 15-PGDH in CCA development by using a mouse model with hydrodynamic tail vein injection of transposase-based plasmids expressing Notch1 intracellular domain and myr-Akt, with or without co-injection of 15-PGDH expression plasmids. Our results reveal that 15-PGDH overexpression effectively prevents CCA development. Through patient data mining and experimental approaches, we provide novel evidences that 15-PGDH is epigenetically silenced by histone methyltransferase G9a. We observe that 15-PGDH and G9a expressions are inversely correlated in both human and mouse CCAs. By using CCA cells and mouse models, we show that G9a inhibition restores 15-PGDH expression and inhibited CCA in vitro and in vivo. Mechanistically, our data indicate that G9a is recruited to 15-PGDH gene promoter via protein-protein interaction with the E-box binding Myc/Max heterodimer. The recruited G9a then silences 15-PGDH gene through enhanced methylation of H3K9. Our further experiments have led to the identification of STAT4 as a key transcription factor involved in the regulation of 15-PGDH by G9a. Collectively, our findings disclose a novel G9a-15PGDH signaling axis which is importantly implicated in CCA development and progression.

Keywords

Cholangiocarcinogenesis; Epigenetics; 15-PGDH; EHMT2; G9a; STAT4

Address correspondence to: Tong Wu, M.D., Ph.D., Department of Pathology and Laboratory Medicine, Tulane University School of Medicine, 1430 Tulane Avenue, SL-79, New Orleans, LA 70112., Tel: 504-988-5210; Fax: 504-988-7862., twu@tulane.edu Or Jinqiang Zhang, Ph.D., Department of Pathology and Laboratory Medicine, Tulane University School of Medicine, 1430 Tulane Avenue, SL-79, New Orleans, LA 70112., Tel: 504-988-5209, jzhang@tulane.edu.

No conflicts of interest exist

Introduction

Cholangiocarcinoma (CCA) is highly aggressive malignancy of the biliary tract with poor prognosis. The incidence and mortality rate of CCA are rising worldwide; currently, there is no effective chemoprevention or systemic therapy(1,2). Being considered as a prototype of cancers associated with inflammation, CCA typically forms in the setting of cholestasis and chronic inflammation that cause reparative injury and biliary epithelial cell proliferation(1–3). Accordingly, primary sclerosing cholangitis (PSC) with chronic inflammation of the biliary tree is the most common predisposing condition for CCA in the Western world(1,2).

Prostaglandin E_2 (PGE_2) is a potent lipid mediator that elicits a wide range of biological effects associated with inflammation and cancer(3). Studies from our group(3–10) and others(11–15) have shown that PGE_2 synthesized by cylooxygenase-2 (COX-2) plays an important role in cholangiocarcinoma progression. Besides PGE_2 biosynthesis, the status of PGE_2 signaling is modulated by 15-hydroxyprostaglandin dehydrogenase (15-PGDH) which catalyzes the oxidation of the 15(S)-hydroxyl group of PGE_2 thus eliminating the biological activity of PGE_2(16,17).

The significance of 15-PGDH in carcinogenesis is attested by the fact that 15-PGDH mRNA and protein levels are significantly decreased in multiple human cancers(18–21), including CCA(5,9). These clinical observations support an important anti-cancer effect of 15-PGDH. In our previous studies(5,9), we have shown that 15-PGDH inhibits CCA cell growth *in vitro* and in xenograft models and that the expression of 15-PGDH in CCA cells is regulated by microRNA-21 and microRNA-26a/b at post-transcriptional level. However, the role of 15-PGDH in CCA development has not been previously investigated and it remains unknown whether and how the expression of the 15-PGDH gene is controlled through transcriptional mechanisms.

Recent studies from our group and others suggest a potentially important role of histone modification in the carcinogenesis and progression of CCA(22–25). Given that epigenetic modification is a key mechanism for the silence of antitumor genes and that CCA lacks clinically significant mutations in the 15-PGDH gene, we consider a high priority to explore whether epigenetic mechanisms may be implicated for regulation of 15-PGDH gene expression in CCA.

In the current study, we provide novel evidence that G9a (also known as Euchromatic histone-lysine N-methyltransferase 2, EHMT2), a H3K9 mono- and di-methyltransferase, is recruited specifically to the promoter of the 15-PGDH gene by the Myc/Max/E-box complex which consequently represses 15-PGDH expression through methylation of H3K9 and prevention of pSTAT4 binding to 15-PGDH promoter element. Our data indicate that these mechanisms are impotently implicated in the regulation of CCA cell growth and invasion, *in vitro* and *in vivo*. Moreover, our experimental findings provide the first evidence that 15-PGDH prevents CCA development which further support 15-PGDH as a key antitumor molecule in cholangiocarcinogenesis.

Materials and Methods

Cell Culture.

Human CCA cell lines CCLP1 and SG231 were cultured in Dulbecco's modified Eagle's medium (Invitrogen, Carlsbad, CA) containing 10% fetal bovine serum (Sigma-Aldrich) and antibiotics (100 U/mL penicillin and 100 μg/mL streptomycin) in a humidified 5% CO_2 incubator at 37°C. Cells within ten passages were used for experiments. All cell lines were latest authenticated by short tandem repeat DNA profiling analysis at ATCC in Oct 2021 and each excluded as having Mycoplasma contamination using the LookOut® Mycoplasma PCR Detection Kit (Sigma-Aldrich) regularly. For establishment of CCA cells with stable depletion of G9a, cells were transfected with pSMP-G9a shRNA or the control vector (pSMP-Luc shRNA). After 48 hours of transfection, the cells were cultured in DMEM medium containing 1 μg/ml Puromycin (Calbiochem, San Diego, CA). The selection medium was replaced every 3 days for the next 4 weeks. Subsequently, distinct colonies of surviving cells were transferred onto 6-well plates and the cultures were maintained under the same selection medium. The efficiency of G9a depletion was verified by Western blotting analysis using anti-G9a antibody.

Mouse CCA Induction by Hydrodynamic Tail Vein Injection.

Eight-week-old mice (C57BL/6J or FVB, purchased from The Jackson Laboratory, Bar Harbor, ME) were anesthetized by isoflurane inhalation through vaporizer to approximately 3–5% for induction and approximately 1–3% for maintenance with oxygen flow to approximately 0.5–1.0 L/min. The anesthetized mouse was placed into the restraining tube. Tail vein injections were performed by using a 27-gauge needle (BD, Franklin Lakes, NJ). Briefly, 10μg pT3-EF1a-NICD, 5μg pT3-EF1a-myr-Akt-HA, 1.25μg pCMV(CAT)T7-SB100 and 15μg of pT3-EF1a-15PGDH or vector control plasmids were diluted in 10% body weight volume (mL) of sterile PBS and injected into a lateral tail vein of mouse within 5–7 seconds. The injected mice were closely monitored and sacrificed at indicated time points. The liver- and body-weights were recorded, and the livers were harvested for further analyses. All the mouse experimental procedures in this study were approved by the Institutional Animal Care and Use Committee (IACUC) of Tulane University.

CCA Xenograft Mouse Model.

Five-week-old male Non-Obese Diabetic CB17-Prkdc/severe combined immunodeficiency (NOD.CB17-Prkdc^{SCID}/J) mice were purchased from The Jackson Laboratory (Bar Harbor, ME). G9a-knockdown or control CCLP1 cell suspensions were mixed with BD Matrigel high concentration matrix (BD Biosciences, San Jose, CA) at 1:1 ratio, and then cell suspension mixtures (1×10^6 cells/10μL) were injected directly into the livers of mice using a Hamilton syringe (model 75 N SYR; Hamilton Co., Reno, NV). The mice were observed closely for tumor formation. At sacrifice, the livers were dissected surgically and the tumor volume was calculated by the following formula: Tumor volume = Wide^2×Length/2.

Chromatin Immunoprecipitation (ChIP).

ChIP assay was performed using a SimpleChIP Enzymatic Chromatin IP kit (Cell Signaling Technology) according to the manufacturer's instructions. Each immunoprecipitation was performed using 1 μg of following antibodies: anti-H3K9me2 (#4658), anti-Myc (#9402), anti-Max (#4739), anti-G9a (#3306) (from Cell Signaling Technology), anti-TFIID (sc-421), anti-c-Ets1 (sc-55581), anti-pSTAT4 (sc-28296), anti-Foxp3 (sc-53876), anti-HNF1A (sc-393925), anti-HNF3a (sc-101058) (from Santa Cruz Biotechnology). Isotype normal IgG was used as a negative control. ChIP primers were designed to amplify the different sites in 15-PGDH promoter regions by real time PCR. The primers are as follows: P_set1 F1, 5'- GAG CAA GGA ACC TCT GTC CC -3'; R1, 5'- TGT CAT CAT CAA CAG GCG CT -3'; P_set2 F2, 5'- TGC TTA GCG GCT TAC CAA CA -3'; R2, 5'- GGG GAA ATG GGA GTT GAG CA -3'; P_set3 F3, 5'- CCT GGT GCT CAC CTG AGT ATT -3'; R3, 5'- ATG GCA ACA TGC TGG GAG AA -3'; P_set4 F4, 5'- CTG GAC AGT GGC AGT GGA AA -3'; R4, 5'- AGC AAG GAC TGA GGT CTA GAG AA -3'. BioRad SsoAdvanced™ Universal SYBR® Green Supermix was used to amplify the target DNA fragments on a Bio-Rad C1000 Thermal Cycler.

Cell Proliferation Assay.

The growth of cells was measured by WST-1 assay. CCA cells (2×10^3 per well) with or without G9a depletion were seeded in 96-well plates at least in triplicate and treated with vehicle control or 15-PGDH inhibitors (sw033291 or $dmPGE_2$). At the indicated time point, the culture medium was removed, and cells were incubated with 100μL of serum-free medium containing 10μL of WST-1 reagents for 2 hours at 37°C. The absorbance of each sample was measured at 450 nm by using an automatic enzyme-linked immunosorbent assay plate reader (VersaMax Microplate Reader; Molecular Devices, Sunnyvale, CA).

Colony Forming Assay.

5×10^3 CCA cells with indicated modification were plated in 10-cm dishes and then the cells were cultured for 14 days to allow colony formation. The colonies were fixed with 100% methanol and then stained with 0.1% crystal violet solution. For sw033291 or $dmPGE_2$ treatment, the indicated cells (5×10^3) were plated in 10-cm dishes and treated with the indicated doses of sw033291, $dmPGE_2$ or vehicle. After 14 days of cell culture, colony formation was determined by crystal violet staining.

Western Blot.

Cells or tissues were lysed in a RIPA buffer (50 mM Tris-HCl pH 8.0, 150 mM NaCl, 5 mM EDTA and 1% NP-40 with protease inhibitor) supplied with phosphatase and protease inhibitors cocktails (Roche, Basel, Switzerland). After being denatured, samples were separated on SDS-PAGE gel and then transferred onto the nitrocellulose membrane (BioRad). The milk-blocked blots were incubated with different primary antibodies at 4°C overnight. After 3× washing with PBS-T, blots were incubated with IRDye 800CW or 680LT conjugated secondary antibodies (LI-COR Biosciences, Lincoln, Ne) and scanned using LI-COR Odyssey Imaging system. The following primary antibodies were used: anti-15PGDH (#160615) from Cayman Chemical, anti-Myc (#9402), anti-

pAkt (#9271), anit-G9a (#3306), anti-H3K9me2 (#4658), anti-STAT4 (#2653) from Cell Signaling Technology, anti-GAPDH (#G8795), anti-Flag (#F3165), anti-β-actin (#A5316) from Sigma-Aldrich, and anti-pSTAT4 (sc-28296) from Santa Cruz Biotechnology.

Thymidine Incorporation Assay.

Thymidine Incorporation Assays were performed using Click-iT™ EdU Alexa Fluor™ 594 Imaging Kit from ThermoFisher Scientific according to the manufacture manual. Briefly, CCA cells with or without G9a depletion were incubated with sw033291 (5 μM), $dmPGE_2$ (5 μM) or vehicle control for 24 hours. After that, cells were incubated with 5 μM EdU (5-ethynyl-2'-deoxyuridine) in serum-free DMEM medium for 24 hours. Then cells were fixed by 3.7% formaldehyde in PBS, followed by detection of incorporated EdU with Alexa 594-labeled azide according to the manual. Nuclei were counterstained by Hoechst 33342.

Bioinformatics Analysis.

Microarray datasets GSE76297 for CCA and non-tumor liver samples gene expression generated by Affymetrix Human Transcriptome Array 2.0 array platform were identified and downloaded from GEO (Gene Expression Omnibus of NCBI). The raw data were processed using oligo and related R packages with Robust Multi-array Average approach for background normalization as per the package instruction. Heatmap was generated by using R package ComplexHeatmap. For transcription factor binding sites identification, 15-PGDH gene upstream sequence (−2000 to +1) was put into algorithm PROMO as a query sequence to search for potential binding sites of putative transcription factors(26).

Statistical Analysis.

Results are presented as mean ± SD from a minimum of 3 replicates. Difference between groups was evaluated by SPSS 19.0 statistical software (IBM, Armonk, NY) with one-way analysis of variance, repeated measure analysis of generalized linear model or Wilcoxon signed-rank test. A p-value < .05 was considered as statistically significant.

Results

15-PGDH prevents cholangiocarcinoma development.

Studies from our lab have shown that 15-PGDH inhibits the growth of CCA cells in vitro and in xenograft models(5,9), although the impact of 15-PGDH on CCA development is not known prior to the current study. We sought to further determine the role of 15-PGDH in CCA development by employing a mouse model of CCA induction via hydrodynamic tail vein injection of sleeping beauty (SB) transposase-based plasmids expressing Notch1 intracellular domain (NICD) and constitutively active Akt as previously described(27). To this end, we constructed a transposase-based 15-PGDH plasmid and co-injected it hydrodynamically with NICD and Akt plasmids into wild type mice. As shown in Figure 1A, while hydrodynamic tail vein injection of NICD/Akt/SB vectors rapidly induced the development of CCA, we observed that mice injected with 15-PGDH in combination with NICD/Akt/SB plasmids (15-PGDH group) developed fewer and smaller tumor nodules when compared with the control mice (injected with control vector in combination with NICD/Akt/SB). The mice in the 15-PGDH group showed significantly lower liver-to-body

weight ratios and better survivals when compared with the mice in the control group (Figure 1B and 1C). Immunohistochemical staining for the cell proliferation marker Ki67 showed lower percentages of Ki67-positive cells in 15-PGDH overexpressed tumors than in control tumors (Figure 1D). Immunoblotting analysis confirmed successful expression of the injected plasmids in the liver tumor tissues (Figure 1E). These findings demonstrate that 15-PGDH overexpression effectively prevents CCA development, and the results establish an important tumor inhibiting role of 15-PGDH in cholangiocarcinogenesis.

The histone methyltransferase G9a is implicated in regulation of 15-PGDH in CCA

Epigenetic gene silencing is one of the key mechanisms underlying dysregulation of tumor-suppressor genes in cancers(28,29). For the regulation of 15-PGDH expression, previous studies have reported a potential role of 15-PGDH promoter hypermethylation in gastric and colon cancer cells(30,31). In our system, we treated human CCA cells (CCLP1) with the DNA methyltransferase inhibitor 5-Aza-2′-deoxycytidine (5-Aza-CdR) and observed that the level of 15-PGDH expression in CCLP1 cells was not altered by (5-Aza-CdR) treatment (Supplementary Figure S1A). In parallel, we analyzed DNA-methylation and corresponding RNA-sequencing data of CCA patients from TCGA-CHOL database (including 9 non-tumor tissues and 36 CCA tissues). Our analysis indicate that 38.9% (14/36) patients have consistent hypermethylation of CpG island located around the transcription starting site of 15-PGDH gene (denoted by Composite Element cg00906130, cg02822257, cg07372795 and cg11073923 in Infinium HumanMethylation450 BeadChip). However, the hypermethylation status of the indicated CpG island have little impacts on 15-PGDH mRNA level in CCA tissues, as indicated by the negligible correlations between the methylation levels (denoted by beta-scores) of these four elements and 15-PGDH mRNA levels in CCA patients' tissues (Supplementary Figure S1B). These findings suggest that DNA methylation does not appear to represent a predominant mechanism for regulation of 15-PGDH gene expression in CCA.

Our data presented in the current study provide novel evidence for an important role of the histone methyltransferase G9a in regulation of 15-PGDH gene expression in CCA. We analyzed the expression levels of all 53 known human histone methyltransferases (HMTs)(32) in CCA and non-tumor tissues of dataset GSE76297, which comprises gene expression data from 91 intrahepatic CCA and 92 adjacent non-tumor tissues (including 90 tumor-nontumor tissue pairs)(33). We observed that 22 HMTs were significantly increased (>1.2 folds) in CCA tissues compared with non-tumor tissues (as shown in Figure 2A and Supplementary Table 1), which include G9a. Our analyses indicate that G9a is the most negatively correlated HMT with 15-PGDH in patients' tissues (Figure 2B) after assessing the correlation between the mRNA levels of 15-PGDH and these 22 increased HMTs. The negative correlation of these two mRNAs was further verified by using additional dataset GSE107943, which comprises gene expression data from 30 CCA and 27 adjacent non-tumor tissues (including 27 tumor-nontumor tissue pairs)(34) (Figure 2B).

Inhibition of G9a enhances the expression of 15-PGDH in CCA cells

Consistent with the above-described results in human data, we detected a noticeable reduction of 15-PGDH and a significant increase of G9a in mouse CCA induced by hydrodynamic tail vein injection of NICD/Akt/SB vectors (Figure 2C, 2D). In our initial

study describing the role of G9a in CCA(25), we showed that treatment with the G9a specific inhibitor, UNC0642, significantly inhibited CCA growth and reduced tumor burden in NICD/Akt-injected mouse model(25). Using the CCA tissues derived from those mice for further immunoblotting, we observed that inhibition of G9a by UNC0642 increased the expression of 15-PGDH in CCA tissues (Figure 2E).

We next assessed the effect of G9a on 15-PGDH expression in cultured human CCA cells (CCLP1 and SG231) transfected with G9a shRNA plasmid or treated with the G9a inhibitor UNC0642. Successful inhibition of G9a histone methyltransferase activity by G9a shRNA or UNC0642 was reflected by decline of H3K9me2 levels (Figure 2F, 2G). Western blotting analysis indicate that G9a depletion by shRNA or G9a inhibition by UNC0642 increased the expression of 15-PGDH in CCA cells (Figure 2F, 2G). These findings demonstrate an important role of G9a for suppression of 15-PGDH expression in CCA cells.

The role of 15-PGDH in G9a-regulated CCA cell growth

Next, we sought to investigate whether G9a depletion would impact tumorigenic potential of CCLP1 cells *in vivo*. For this purpose, 1×10^6 CCLP1 cells with or without G9a knockdown were mixed with matrigel and inoculated orthotopically into the livers of SCID mice through liver injection. We observed that, by 7 weeks post-injection, the recipient mice receiving G9a depleted CCLP1 cells developed much smaller tumor nodules when compared with the mice receiving control CCLP1 cells (Figure 3A and 3B). Given that PGE_2 plays an important role in tumor invasion and metastasis(35), we further examined the intrahepatic metastasis in the tumor-adjacent liver tissues. We observe that the mice receiving G9a-depleted CCLP1 cells exhibited significantly less metastatic foci when compared with the group receiving control CCLP1 cells (Figure 3C). Western blotting assays confirmed reduced G9a and elevated 15-PGDH protein levels in tumors formed by G9a-depleted CCLP1 cells (Figure 3D).

To further assess the functional implication of 15-PGDH in G9a-mediated CCA cell growth, we evaluated whether 15-PGDH inhibition could rescue the inhibition of CCA cell growth induced by G9a-depletion. For this purpose, we utilized CCA cell lines with stable G9a knockdown (as shown above in Figure 2F, successful reduction of G9a protein by shRNA in the stable cell lines were verified by immunoblotting analysis). We observed that G9a depletion by shRNA significantly decreased the proliferation of CCA cells when compared with their corresponding control cells (Figure 4A and 4B). G9a knockdown also reduced the clonogenicity of CCA cells (Figure 4C). Importantly, treatment with two separate 15-PGDH inhibitors, including 16,16-dimethyl PGE_2 (an agonist of prostaglandin E receptor and a competitive inhibitor of 15-PGDH) or sw033291 (a noncompetitive inhibitor of 15-PGDH), rescued the proliferation and clonogenic capability of G9a-depleted CCA cells (Figure 4A, 4B and 4C). These results, along with the data that G9a depletion increased 15-PGDH levels in mouse CCA (Figure 3D), demonstrate the role of 15-PGDH in G9a-mediated CCA progression.

Myc/Max complex recruit G9a to methylate H3K9 in the promoter of 15-PGDH

Given that G9a catalyzes the mono- and di-methylation of H3K9 with high specificity(36), we further performed chromatin immunoprecipitation (ChIP) assay by using anti-H3K9me2 antibody and primer pairs specific for 15-PGDH promoter. We observed that 15-PGDH promoter fragments were greatly enriched by anti-H3K9me2, and this enrichment was repressed significantly by UNC0642 treatment (Figure 5A, 5B). Thus, the H3K9 residues in 15-PGDH promoter region are heavily di-methylated, which support the role of G9a in the silencing of 15-PGDH gene expression. Our findings suggest that G9a inhibits 15-PGDH expression in CCA through modifying the methylation status of H3K9 in the promoter of 15-PGDH gene.

Next, we sought to further investigate how G9a was specifically recruited to the promoter region of the 15-PGDH gene. Recently, Dingar et al had explored Myc/Max interactome systematically by using BioID (Proximity-dependent biotin identification)-mass spectrometry in multiple cell types; it came to our attention that G9a is included as a high confidence interactor with Myc/Max heterodimer(37,38). Through bioinformatics analyses, we have found that there are four putative Myc/Max-bound E-box elements (CAGCTG×3 and CACCTG×1) in human 15-PGDH promoter region (−2000 to +1)(39), as indicated in Figure 5A. Based on these observations, we postulate that Myc/Max heterodimer could mediate the recruiting of G9a to 15-PGDH promoter. To validate this hypothesis, we performed ChIP experiments with anti-Myc, anti-Max or anti-G9a antibodies in CCA cells. Our data showed that the 15-PGDH promoter fragments were significantly enriched by all of the above three antibodies (Figure 5C and 5D). These observations indicate the association of these proteins with the 15-PGDH promoter. Next, we carried out co-immunoprecipitation assays to determine the association of Myc/Max with G9a in CCA cells. As shown in Figure 5E, these three proteins form complex in CCLP1 cells. Taken together, our findings suggest that Myc/Max complex recruits G9a to the promoter region of the 15-PGDH gene which leads to methylation of the H3K9 residues and silencing of 15-PGDH gene expression.

G9a-mediated H3K9 methylation prevents the binding of pSTAT4 to 15-PGDH gene promoter

Our next goal was to identify transcription factors (TFs) that can activate 15-PGDH transcription and can be inhibited by G9a in CCA cells. We performed bioinformatics analyses using PROMO algorithm with strictest screening criteria(26); this approach led to the identification of six TFs (TFIID, c-Ets-1, STAT4, Foxp3, HNF1A and HNF3a) which have putative binding sites located at the upstream (−2000 to +1) of the human 15-PGDH gene (Figure 6A). We then carried out ChIP assay with a set of 4 primer pairs to evaluate the effects of G9a-depletion on the interactions between the predicted TFs and the 15-PGDH gene promoter. While the ChIP results revealed the binding of TFIID, c-Ets-1 and pSTAT4 to the 15-PGDH promoter, we observed that only pSTAT4 binding was significantly boosted by G9a knockdown in CCLP1 cells (with consistent phosphorylation status of STAT4), which was further verified in SG231 cells (Figure 6B, 6C, 6D and Supplementary Figure S2A). We observed that STAT4 protein levels were significantly decreased in human CCA tissues when compared with the non-tumor tissues (Supplementary Figure S2B). Based on these findings, we evaluated whether forced overexpression of STAT4 would enhance

15-PGDH expression in CCA cells. Indeed, we observed a considerable rise of 15-PGDH protein level in CCLP1 cells transfected with STAT4-expressing plasmid (Figure 6E). To further determine whether there was a correlation between STAT4 and 15-PGDH in CCA tissues, we performed co-expression analyses between these two genes in CCA patients' tissues from dataset GSE76297; this analysis revealed positive correlation between STAT4 and 15-PGDH in human CCA tissues (Figure 6F). These observations, in combination with the data that G9a inhibition decreases H3K9 methylation level (Figure 2E–G) and reduces H3K9me2 association with 15-PGDH promoter (Figure 5B) suggest that G9a-mediated H3K9 methylation prevents the binding of pSTAT4 to its target element in the 15-PGDH promoter.

Taken together, our findings disclose a novel mechanism for regulation of 15-PGDH gene expression in CCA cells: G9a is recruited to 15-PGDH promoter by Myc/Max/E-box complex and the recruited G9a catalyzes H3K9 methylation which prevents the binding of transcription factors (i.e., pSTAT4) leading to transcriptional repression of 15-PGDH gene expression (outlined in Figure 7). Our data support an important role of this novel regulatory mechanism in cholangiocarcinogenesis.

Discussion

Prostaglandin E2 (PGE_2) synthesis involves cyclooxygenase-1 and -2 (COX-1 and -2). While COX-1 is constitutively active in most tissues to maintain physiologic level of PGE_2, COX-2 is highly inducible in various tissues by pro-inflammatory and mitogenic stimuli, including cytokines and growth factors(3,40). Compelling evidence has shown that COX-2-derived PGE_2 plays an important role in promoting cell survival, stimulating cell proliferation and motility, inducing angiogenesis, and suppressing immune surveillance(3,4,6,7,11–13,15,17,41,42). Studies from several laboratories have shown that PGE_2 synthesized by cylooxygenase-2 (COX-2) plays an important role in cholangiocarcinoma progression(4,6,7,11,12,14,15,41). PGE_2 is known to activate G protein-coupled receptors and then initiates diverse intracellular events in CCA, such as protein kinase activation and proinflammatory cytokines production, which consequently lead to increased cell growth and tumor invasion(3). In addition to the function-based ligand-receptor interaction, COX2/PGE_2 signaling also interacts with other key pathways in CCA, such as iNOS(43), EGFR(8,14), and Wnt/β-catenin pathway(4).

In addition to biosynthesis, PGE_2 level is tightly controlled by its metabolic degradation. The NAD^+-dependent 15-hydroxyprostaglandin dehydrogenase (15-PGDH) catalyzes the oxidation of the 15(S)-hydroxyl group of PGE_2 which leads to inactivation of PGE_2(16,17). Previous studies from our group(5,9) have shown that (i) 15-PGDH mRNA and protein levels are decreased in CCA; (ii) 15-PGDH inhibits CCA cell growth *in vitro* and in xenograft models and (iii) the expression of 15-PGDH in CCA cells is regulated by microRNA-21 and microRNA-26a at post-transcriptional level. However, the role of 15-PGDH in CCA development has not been previously investigated and it remains unknown whether and how the expression of the 15-PGDH gene is controlled through transcriptional mechanisms.

In the current study, by employing a novel mouse CCA model induced by hydrodynamic tail vein injection of NICD/Akt plasmids, we observed that overexpression of 15-PGDH efficiently prevent CCA development. These experimental findings support 15-PGDH as an important antitumor molecule in cholangiocarcinogenesis. These results, along the existing data on 15-PGDH in CCA, may have important clinical relevance, given that 15-PGDH is much more specific than selective COX-2 inhibitors with respect to PEG2 signaling inhibition. Different from 15-PGDH, whose main metabolic substrates are limited to prostaglandins and eicosanoids(16), selective COX-2 inhibitors may have severe off-target effects by interacting with a broad spectrum of molecules such as cGMP phosphodiesterase, PPARs, NF-κB, Akt, and 15-lipoxygenase-1(3). Our findings suggest that induction of 15-PGDH may represent an effective substitute approach for COX-2 inhibitors treatment in chemoprevention and adjuvant anti-cancer therapy.

Epigenetic modifications are characteristic of all cancers, from apparently normal precursor tissue to advanced metastatic disease, and these epigenetic modifications confer growth advantage upon tumor cells through disrupting the functions of diverse genes(28,29). In the current study, our findings reveal an important epigenetic mechanism for regulation of 15-PGDH expression in CCA cells. Specifically, our results indicate a key role of the histone methyltransferase EHMT2/G9a for inhibition of 15-PGDH gene expression in CCA. The latter assertion is supported by the steady increase of 15-PGDH expression in G9a-depleted CCA cells in culture and in mice; and by the findings from bioinformatics analyses indicating that G9a and 15-PGDH mRNA levels are inversely correlated in human CCA tissues.

In addition to epigenetic modifications, genetic mutation is the other key mechanism that silences tumor suppressors in cancer. However, we were unable to identify any mutation in 15-PGDH exons after performing data mining analysis across more than 450 patients with bile tract cancer from various publications based on different high-throughput platforms(44,45). Instead, our findings in the current study all point toward the notion that G9a-mediated histone methylation is a key mechanism for 15-PGDH repression in CCA.

The chromatins of many tumor suppressor genes in cancer are marked by both DNA methylation and histone H3K9 methylation. Although the exact relationship between these epigenetic modifications is not fully elucidated, it is becoming clear that histone methylation occurs during the initial phases of gene silencing in cancer, and DNA methylation might then spread over the gene promoter in the process of cell division to maintain associated histone modifications and gene silence(28,46,47). Compelling evidences in various experimental systems with deficient DNA methyltransferase function have already shown that G9a alone can induce gene silence through methylating H3K9(46–48). For example, H3K9 methylation associated with silencing of $p16^{INK4}$ gene can occur prior to and independently of DNA methylation in colon cancer(47); G9a can block Oct-3/4 gene reactivation through methylating H3K9 independent of its Dnmt3a/b recruiting function in embryonic cells(48). These facts are in agreement with our observation that G9a depletion/inhibition effectively alters 15-PGDH expression, while inhibition of DNA methyltransferase by 5-Aza-CdR exhibits little effect on 15-PGDH level in CCA cells. All of these phenomena fit well with the view that G9a is a master structural regulator

with an important role in early development and carcinogenesis(46,48). In this context, our experimental findings are noteworthy as they provide further evidence in support of G9a as a promising epigenetic oncotarget for developing inhibitors as anticancer therapeutic drugs(49). In this context, is worth mentioning that we have demonstrated in our previous study that the G9a inhibitor UNC0642 effectively prevents the development of CCA induced by hydrodynamic tail vein injection of NICD and Akt plasmids in mice(25).

Another novel aspect of this study is the identification of a functional connection between STAT4 and 15-PGDH in CCA. According to the Human Protein Atlas database, increased STAT4 is considered as a favorable prognostic maker in most types of human cancer(50). While previous studies have focused on the activation of STAT4 signaling by cytokines in immunocytes, the detailed functional role of STAT4 in cancer cells has not been fully considered. Our results presented in this study reveal a possible mechanism underlying tumor-inhibiting role of STAT4 in cancer cells, which is to up-regulate the transcription of its target gene 15-PGDH. These facts support a tumor-inhibitory role of STAT4 in cholangiocarcinoma.

In addition, we would like to reiterate the inhibiting effect of c-Myc on 15-PGDH in cholangiocarcinoma. In our previous study, we have demonstrated that c-Myc is involved in 15-PGDH repression through regulating miR-26a/b and their host genes(9). Here, we describe a separate novel mechanism underlying the repressing effect of c-Myc on 15-PGDH expression. Specifically, our data demonstrate that Myc/Max, when binding to E-box elements located in the promoter of 15-PGDH can recruit G9a to form a DNA-protein complex. Then, this complex drives the transcription repression of 15-PGDH through methylating adjacent H3K9 residues.

In summary, our findings presented in the current study disclose a novel mechanism of epigenetic regulation of 15-PGDH by G9a in CCA. Therefore, disrupting the c-Myc-elicited, G9a-mediated transcriptional repression axis and/or inducing the re-expression of 15-PGDH may represent a potentially effective strategy for the chemoprevention and adjuvant therapy of cholangiocarcinoma.

Supplementary Material

Refer to Web version on PubMed Central for supplementary material.

Financial Support:

This work was supported by the National Institutes of Health grants CA102325, CA219541, CA226281, and Department of Defense grant CA180361.

List of abbreviations:

CCA	Cholangiocarcinoma
15-PGDH	NAD^+-dependent 15-hydroxyprostaglandin dehydrogenase
EHMT2/G9a	Euchromatic Histone Lysine Methyltransferase 2

NICD	Notch1 intracellular domain
PGE_2	Prostaglandin E_2
COX	Cyclooxygenase
HMTs	Histone Methyltransferases
STAT4	Signal Transducer and Activator of Transcription 4

References

1. Banales JM, Marin JJG, Lamarca A, Rodrigues PM, Khan SA, Roberts LR, et al. Cholangiocarcinoma 2020: the next horizon in mechanisms and management. Nat Rev Gastroenterol Hepatol 2020;17:557–88 [PubMed: 32606456]
2. Rizvi S, Khan SA, Hallemeier CL, Kelley RK, Gores GJ. Cholangiocarcinoma - evolving concepts and therapeutic strategies. Nat Rev Clin Oncol 2018;15:95–111 [PubMed: 28994423]
3. Wu T Cyclooxygenase-2 and prostaglandin signaling in cholangiocarcinoma. Biochim Biophys Acta 2005;1755:135–50 [PubMed: 15921858]
4. Lim K, Han C, Xu L, Isse K, Demetris AJ, Wu T. Cyclooxygenase-2-derived prostaglandin E2 activates beta-catenin in human cholangiocarcinoma cells: evidence for inhibition of these signaling pathways by omega 3 polyunsaturated fatty acids. Cancer Res 2008;68:553–60 [PubMed: 18199552]
5. Lu L, Byrnes K, Han C, Wang Y, Wu T. miR-21 targets 15-PGDH and promotes cholangiocarcinoma growth. Molecular cancer research : MCR 2014;12:890–900 [PubMed: 24699315]
6. Wu T, Han C, Lunz JG 3rd, Michalopoulos G, Shelhamer JH, Demetris AJ. Involvement of 85-kd cytosolic phospholipase A(2) and cyclooxygenase-2 in the proliferation of human cholangiocarcinoma cells. Hepatology 2002;36:363–73 [PubMed: 12143044]
7. Wu T, Leng J, Han C, Demetris AJ. The cyclooxygenase-2 inhibitor celecoxib blocks phosphorylation of Akt and induces apoptosis in human cholangiocarcinoma cells. Molecular cancer therapeutics 2004;3:299–307 [PubMed: 15026550]
8. Xu L, Han C, Lim K, Wu T. Cross-talk between peroxisome proliferator-activated receptor delta and cytosolic phospholipase A(2)alpha/cyclooxygenase-2/prostaglandin E(2) signaling pathways in human hepatocellular carcinoma cells. Cancer Res 2006;66:11859–68 [PubMed: 17178883]
9. Yao L, Han C, Song K, Zhang J, Lim K, Wu T. Omega-3 Polyunsaturated Fatty Acids Upregulate 15-PGDH Expression in Cholangiocarcinoma Cells by Inhibiting miR-26a/b Expression. Cancer Res 2015;75:1388–98 [PubMed: 25691459]
10. Han C, Leng J, Demetris AJ, Wu T. Cyclooxygenase-2 promotes human cholangiocarcinoma growth: evidence for cyclooxygenase-2-independent mechanism in celecoxib-mediated induction of p21waf1/cip1 and p27kip1 and cell cycle arrest. Cancer Res 2004;64:1369–76 [PubMed: 14973068]
11. Nzeako UC, Guicciardi ME, Yoon JH, Bronk SF, Gores GJ. COX-2 inhibits Fas-mediated apoptosis in cholangiocarcinoma cells. Hepatology 2002;35:552–9 [PubMed: 11870367]
12. Sirica AE, Lai GH, Endo K, Zhang Z, Yoon BI. Cyclooxygenase-2 and ERBB-2 in cholangiocarcinoma: potential therapeutic targets. Seminars in liver disease 2002;22:303–13 [PubMed: 12360423]
13. Sirica AE, Lai GH, Zhang Z. Biliary cancer growth factor pathways, cyclo-oxygenase-2 and potential therapeutic strategies. Journal of gastroenterology and hepatology 2001;16:363–72 [PubMed: 11357901]
14. Yoon JH, Higuchi H, Werneburg NW, Kaufmann SH, Gores GJ. Bile acids induce cyclooxygenase-2 expression via the epidermal growth factor receptor in a human cholangiocarcinoma cell line. Gastroenterology 2002;122:985–93 [PubMed: 11910351]

15. Zhang Z, Lai GH, Sirica AE. Celecoxib-induced apoptosis in rat cholangiocarcinoma cells mediated by Akt inactivation and Bax translocation. Hepatology 2004;39:1028–37 [PubMed: 15057907]
16. Tai HH, Ensor CM, Tong M, Zhou H, Yan F. Prostaglandin catabolizing enzymes. Prostaglandins Other Lipid Mediat 2002;68–69:483–93
17. Palla AR, Ravichandran M, Wang YX, Alexandrova L, Yang AV, Kraft P, et al. Inhibition of prostaglandin-degrading enzyme 15-PGDH rejuvenates aged muscle mass and strength. Science 2021;371
18. Yan M, Rerko RM, Platzer P, Dawson D, Willis J, Tong M, et al. 15-Hydroxyprostaglandin dehydrogenase, a COX-2 oncogene antagonist, is a TGF-beta-induced suppressor of human gastrointestinal cancers. Proc Natl Acad Sci U S A 2004;101:17468–73 [PubMed: 15574495]
19. Ding Y, Tong M, Liu S, Moscow JA, Tai HH. NAD+-linked 15-hydroxyprostaglandin dehydrogenase (15-PGDH) behaves as a tumor suppressor in lung cancer. Carcinogenesis 2005;26:65–72 [PubMed: 15358636]
20. Myung SJ, Rerko RM, Yan M, Platzer P, Guda K, Dotson A, et al. 15-Hydroxyprostaglandin dehydrogenase is an in vivo suppressor of colon tumorigenesis. Proc Natl Acad Sci U S A 2006;103:12098–102 [PubMed: 16880406]
21. Wolf I, O'Kelly J, Rubinek T, Tong M, Nguyen A, Lin BT, et al. 15-hydroxyprostaglandin dehydrogenase is a tumor suppressor of human breast cancer. Cancer Res 2006;66:7818–23 [PubMed: 16885386]
22. Nakagawa S, Sakamoto Y, Okabe H, Hayashi H, Hashimoto D, Yokoyama N, et al. Epigenetic therapy with the histone methyltransferase EZH2 inhibitor 3-deazaneplanocin A inhibits the growth of cholangiocarcinoma cells. Oncol Rep 2014;31:983–8 [PubMed: 24337160]
23. Kwon H, Song K, Han C, Zhang J, Lu L, Chen W, et al. Epigenetic Silencing of miRNA-34a in Human Cholangiocarcinoma via EZH2 and DNA Methylation: Impact on Regulation of Notch Pathway. Am J Pathol 2017;187:2288–99 [PubMed: 28923203]
24. O'Rourke CJ, Munoz-Garrido P, Aguayo EL, Andersen JB. Epigenome dysregulation in cholangiocarcinoma. Biochim Biophys Acta Mol Basis Dis 2018;1864:1423–34 [PubMed: 28645654]
25. Ma W, Han C, Zhang J, Song K, Chen W, Kwon H, et al. The Histone Methyltransferase G9a Promotes Cholangiocarcinogenesis Through Regulation of the Hippo Pathway Kinase LATS2 and YAP Signaling Pathway. Hepatology 2020
26. Messeguer X, Escudero R, Farre D, Nunez O, Martinez J, Alba MM. PROMO: detection of known transcription regulatory elements using species-tailored searches. Bioinformatics 2002;18:333–4 [PubMed: 11847087]
27. Fan B, Malato Y, Calvisi DF, Naqvi S, Razumilava N, Ribback S, et al. Cholangiocarcinomas can originate from hepatocytes in mice. The Journal of clinical investigation 2012;122:2911–5 [PubMed: 22797301]
28. Baylin SB, Ohm JE. Epigenetic gene silencing in cancer - a mechanism for early oncogenic pathway addiction? Nature reviews Cancer 2006;6:107–16 [PubMed: 16491070]
29. Timp W, Feinberg AP. Cancer as a dysregulated epigenome allowing cellular growth advantage at the expense of the host. Nature reviews Cancer 2013;13:497–510 [PubMed: 23760024]
30. Backlund MG, Mann JR, Holla VR, Shi Q, Daikoku T, Dey SK, et al. Repression of 15-hydroxyprostaglandin dehydrogenase involves histone deacetylase 2 and snail in colorectal cancer. Cancer Res 2008;68:9331–7 [PubMed: 19010907]
31. Thiel A, Ganesan A, Mrena J, Junnila S, Nykanen A, Hemmes A, et al. 15-hydroxyprostaglandin dehydrogenase is down-regulated in gastric cancer. Clinical cancer research : an official journal of the American Association for Cancer Research 2009;15:4572–80 [PubMed: 19584167]
32. Chandrashekar DS, Bashel B, Balasubramanya SAH, Creighton CJ, Ponce-Rodriguez I, Chakravarthi B, et al. UALCAN: A Portal for Facilitating Tumor Subgroup Gene Expression and Survival Analyses. Neoplasia 2017;19:649–58 [PubMed: 28732212]
33. Chaisaingmongkol J, Budhu A, Dang H, Rabibhadana S, Pupacdi B, Kwon SM, et al. Common Molecular Subtypes Among Asian Hepatocellular Carcinoma and Cholangiocarcinoma. Cancer cell 2017;32:57–70 e3 [PubMed: 28648284]

34. Ahn KS, Kang KJ, Kim YH, Kim TS, Song BI, Kim HW, et al. Genetic features associated with (18)F-FDG uptake in intrahepatic cholangiocarcinoma. Ann Surg Treat Res 2019;96:153–61 [PubMed: 30941318]
35. Greenhough A, Smartt HJ, Moore AE, Roberts HR, Williams AC, Paraskeva C, et al. The COX-2/PGE2 pathway: key roles in the hallmarks of cancer and adaptation to the tumour microenvironment. Carcinogenesis 2009;30:377–86 [PubMed: 19136477]
36. Tachibana M, Sugimoto K, Fukushima T, Shinkai Y. Set domain-containing protein, G9a, is a novel lysine-preferring mammalian histone methyltransferase with hyperactivity and specific selectivity to lysines 9 and 27 of histone H3. The Journal of biological chemistry 2001;276:25309–17 [PubMed: 11316813]
37. Tu WB, Shiah YJ, Lourenco C, Mullen PJ, Dingar D, Redel C, et al. MYC Interacts with the G9a Histone Methyltransferase to Drive Transcriptional Repression and Tumorigenesis. Cancer cell 2018;34:579–95 e8 [PubMed: 30300580]
38. Dingar D, Tu WB, Resetca D, Lourenco C, Tamachi A, De Melo J, et al. MYC dephosphorylation by the PP1/PNUTS phosphatase complex regulates chromatin binding and protein stability. Nature communications 2018;9:3502
39. Allevato M, Bolotin E, Grossman M, Mane-Padros D, Sladek FM, Martinez E. Sequence-specific DNA binding by MYC/MAX to low-affinity non-E-box motifs. PloS one 2017;12:e0180147 [PubMed: 28719624]
40. Wang D, Dubois RN. Prostaglandins and cancer. Gut 2006;55:115–22 [PubMed: 16118353]
41. Endo K, Yoon BI, Pairojkul C, Demetris AJ, Sirica AE. ERBB-2 overexpression and cyclooxygenase-2 up-regulation in human cholangiocarcinoma and risk conditions. Hepatology 2002;36:439–50 [PubMed: 12143054]
42. Hayashi N, Yamamoto H, Hiraoka N, Dono K, Ito Y, Okami J, et al. Differential expression of cyclooxygenase-2 (COX-2) in human bile duct epithelial cells and bile duct neoplasm. Hepatology 2001;34:638–50 [PubMed: 11584358]
43. Ishimura N, Bronk SF, Gores GJ. Inducible nitric oxide synthase upregulates cyclooxygenase-2 in mouse cholangiocytes promoting cell growth. Am J Physiol Gastrointest Liver Physiol 2004;287:G88–95 [PubMed: 14977638]
44. Farshidfar F, Zheng S, Gingras MC, Newton Y, Shih J, Robertson AG, et al. Integrative Genomic Analysis of Cholangiocarcinoma Identifies Distinct IDH-Mutant Molecular Profiles. Cell Rep 2017;18:2780–94 [PubMed: 28297679]
45. Zou S, Li J, Zhou H, Frech C, Jiang X, Chu JS, et al. Mutational landscape of intrahepatic cholangiocarcinoma. Nature communications 2014;5:5696
46. Jones PA, Baylin SB. The fundamental role of epigenetic events in cancer. Nat Rev Genet 2002;3:415–28 [PubMed: 12042769]
47. Bachman KE, Park BH, Rhee I, Rajagopalan H, Herman JG, Baylin SB, et al. Histone modifications and silencing prior to DNA methylation of a tumor suppressor gene. Cancer cell 2003;3:89–95 [PubMed: 12559178]
48. Epsztejn-Litman S, Feldman N, Abu-Remaileh M, Shufaro Y, Gerson A, Ueda J, et al. De novo DNA methylation promoted by G9a prevents reprogramming of embryonically silenced genes. Nat Struct Mol Biol 2008;15:1176–83 [PubMed: 18953337]
49. Soumyanarayanan U, Dymock BW. Recently discovered EZH2 and EHMT2 (G9a) inhibitors. Future Med Chem 2016;8:1635–54 [PubMed: 27548656]
50. Uhlen M, Fagerberg L, Hallstrom BM, Lindskog C, Oksvold P, Mardinoglu A, et al. Proteomics. Tissue-based map of the human proteome. Science 2015;347:1260419 [PubMed: 25613900]

Implications:

The current study describes a novel G9a-15PGDH signaling axis which is importantly implicated in cholangiocarcinoma (CCA) development and progression.

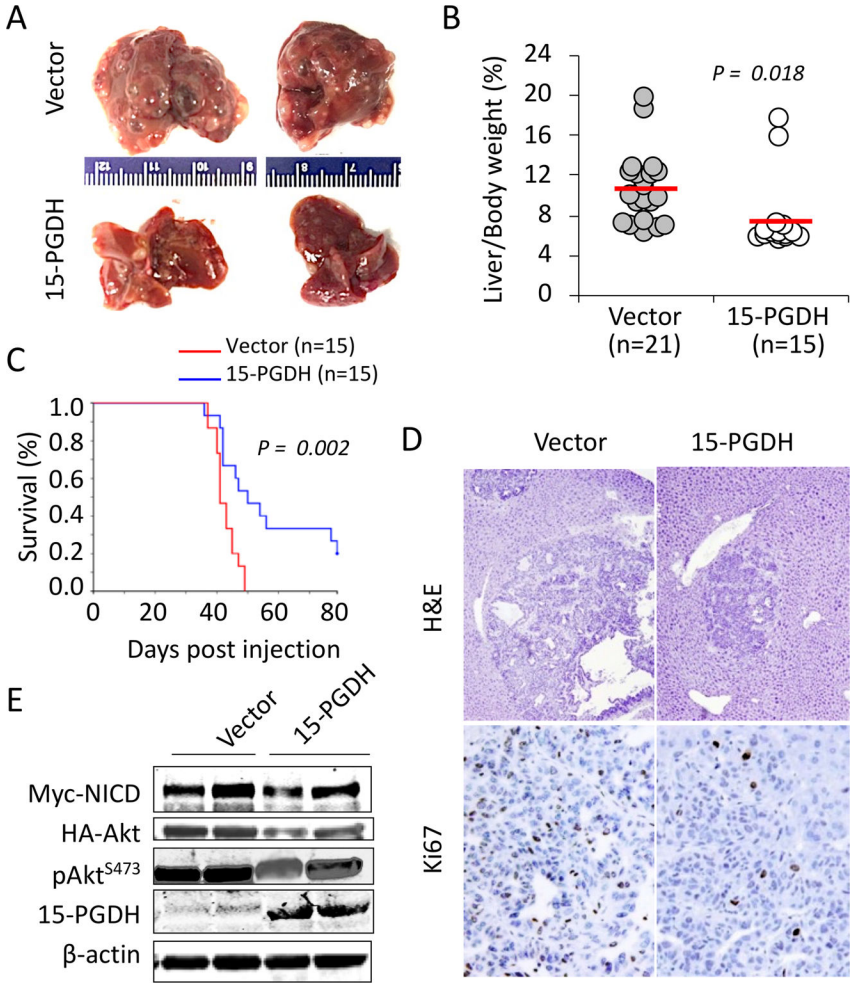

Figure 1. 15-PGDH inhibits CCA tumor development in vivo.

(**A, B**) mouse intrahepatic CCAs induced by hydrodynamic injection of NICD (with N-terminal Myc tag), myr-Akt (with C-terminal HA tag) and sleeping beauty transposase plasmids (NICD/Akt/SB) in combination with 15-PGDH expressing plasmid or control vector. Panel A shows the representative mouse livers of each group by 4.5 weeks after hydrodynamic injection. The liver/body ratios of mice are shown in (B). Red bars indicating mean value of each group. (**C**) Kaplan-Meier curve demonstrates that mice co-injected with NICD/Akt/SB/15-PGDH plasmids have better survival than mice co-injected with NICD/Akt/SB/Vector plasmids. (**D**) Representative images of H&E stains (40×) and Ki-67 immunostaining (100×) of CCA tissues from mice 4.5 weeks after hydrodynamic injection of NICD/Akt/SB in combination with 15-PGDH expressing or control plasmids. (**E**) Western blots verified the levels of indicated proteins in CCA tissues from vector control group and 15-PGDH group of mice.

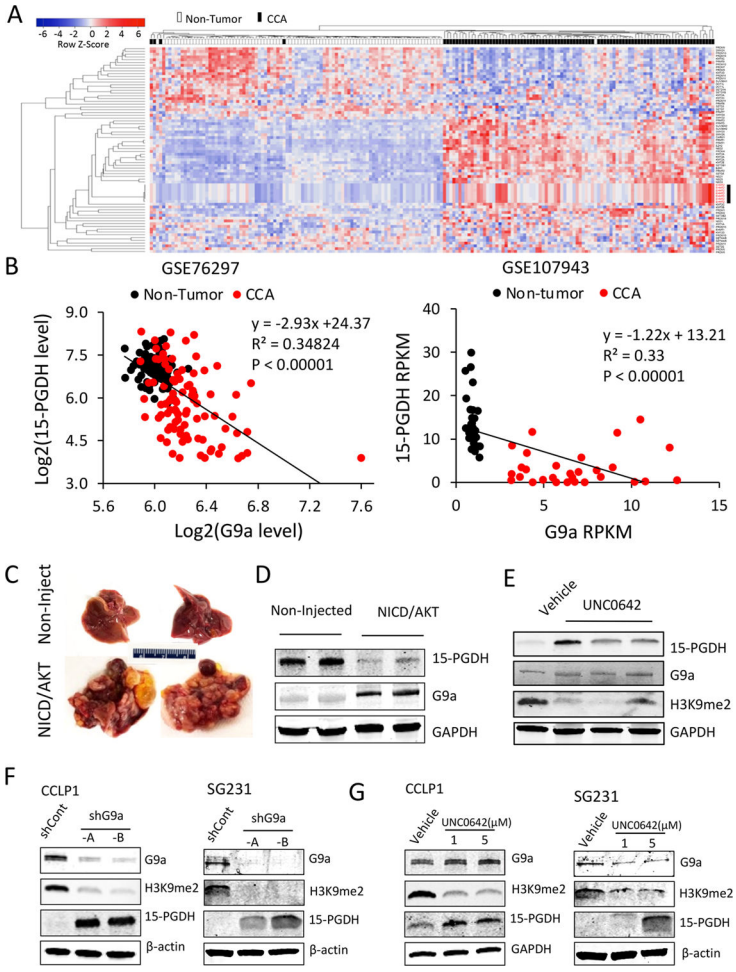

Figure 2. G9a regulates 15-PGDH level in CCA.

(**A**) Heatmap shows the mRNA levels of 53 known human histone methyltransferases in 91 CCA and 92 non-tumor tissues (GSE76297), 22 of which were found significantly increased in CCA, including EHMT2/G9a (its seven probes were indicated black bar on the right). (**B**) 15-PGDH and G9a expressions are inversely correlated in CCA patient tissues. (**C**) Representative gross photographs of livers from mice with or without hydrodynamic tail vein injection of NICD/Akt/SB plasmids. (**D**) Immunoblots show the decreased 15-PGDH and increased G9a levels in mouse livers as shown in (C). (**E**) Mice receiving hydrodynamic tail vein injection of NICD/Akt/SB plasmids were treated with 2.5 mg/kg G9a inhibitor UNC0642 every other day through intraperitoneal injection. The treatment began 1 week after injection and continued for 3 weeks. Five weeks after injection, the animals were sacrificed, and the livers were harvested for immunoblotting with indicated antibodies. (**F, G**) G9a knockdown by shRNA (F) or inhibition by UNC0642 treatment for 48 hours (G) increased 15-PGDH level in CCLP1 and SG231 cells.

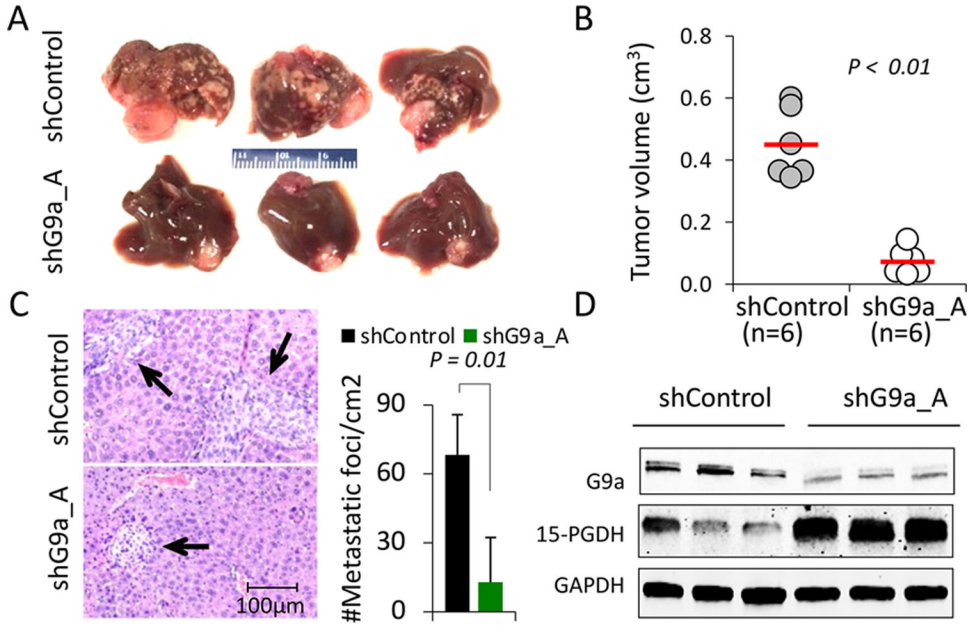

Figure 3. G9a knockdown inhibits CCA growth and metastasis *in vivo*.

(**A, B**) G9a knockdown or control CCLP1 cells were orthotopically inoculated into the livers of SCID mice, and the livers were recovered 7 weeks later. Representative livers of each group are shown in (A), and the tumor volumes ($V = Wide^2 \times Length/2$) data are shown in (B) with red bars indicating mean volumes of each group. (**C**) Representative H&E staining show the intrahepatic metastatic foci (indicated by arrows) in tumor adjacent liver tissues from mice inoculated with G9a knockdown or control CCLP1 cells. The average numbers of intrahepatic metastatic foci in each group are shown in the chart at the right panel. (**D**) Immunoblotting verified the inverse correlation of 15-PGDH and G9a protein levels in tumor tissues shown in (A).

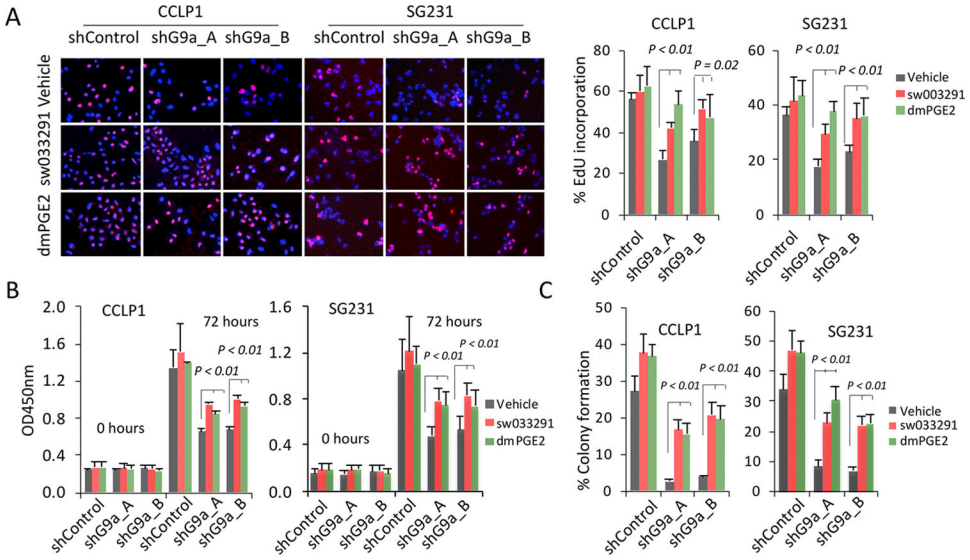

Figure 4. 15-PGDH inhibitors partly restore cell growth in G9a-depleted CCA cells.

Thymidine incorporation assays (**A**), WST-1 assays (**B**) and colony forming assays (**C**) showed that G9a knockdown by shRNA prevents CCLP1and SG231 cell proliferation and colony forming capacity, which can be partially restored by treatment with the 15-PGDH specific inhibitors, sw033291 (5 μM) or 16,16-Dimethyl-PGE_2 (5 μM).

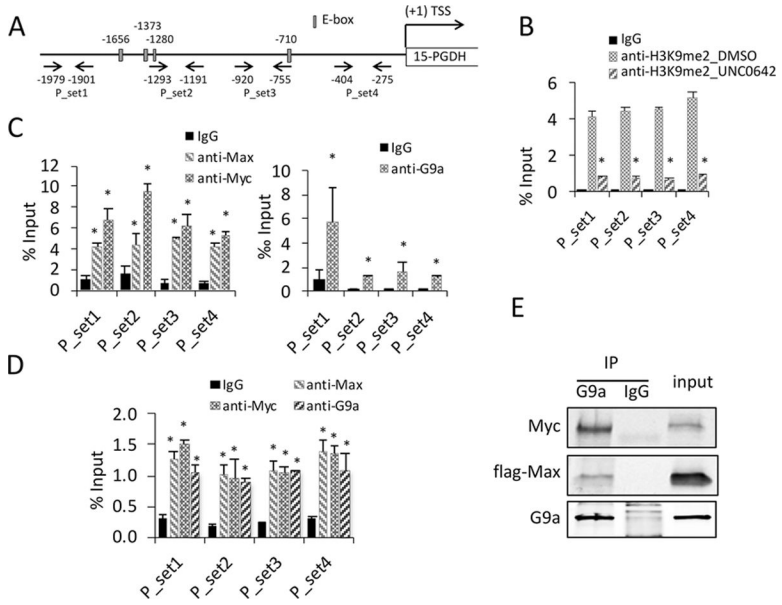

Figure 5. Myc/Max Complex recruit G9a to repress 15-PGDH transcription.

(**A**) Predicted Myc/Max binding sites (E-box) in the promoter region (−2000 to +1) of human 15-PGDH gene and ChIP primer scheme. The numbers indicate the starting points of each element. (**B**) ChIP assays validated the methylation of H3K9 in 15-PGDH promoter, and the H3K9 methylation was inhibited by UNC0642 in CCLP1 cells. (**C**, **D**) ChIP results demonstrate the binding of G9a, Myc and Max to 15-PGDH gene promoter region in CCLP1 (C) and SG231 (D) cells. (**E**) Immunoprecipitation results verified the interaction of Myc, Max and G9a in CCLP1 cells (transfected with Max-expressing plasmids). * $p < 0.01$ vs. corresponding control.

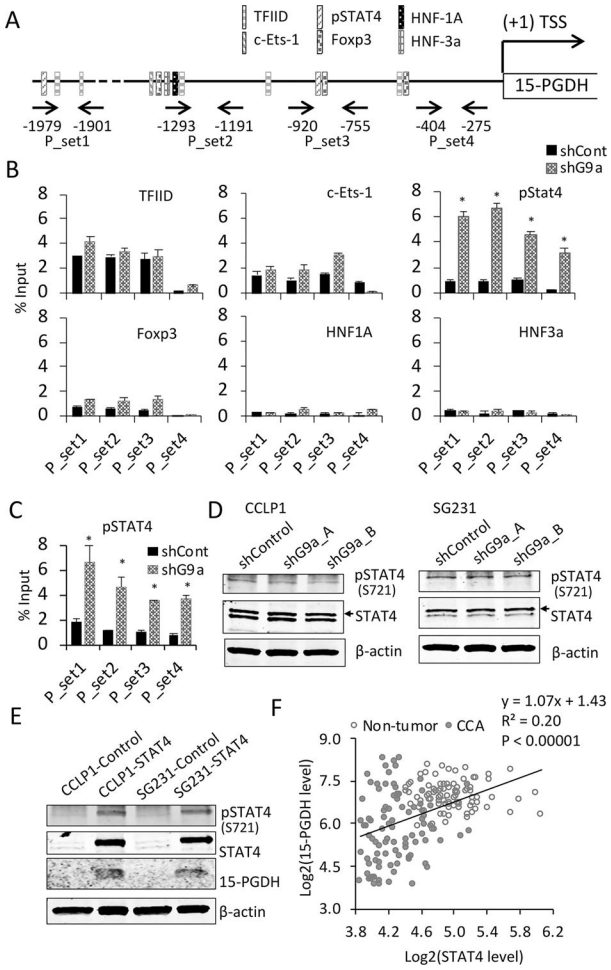

Figure 6. STAT4 is involved in the silencing of 15-PGDH gene by G9a.

(**A**) Predicted TFs binding sites in the promoter region of human 15-PGDH gene and ChIP primer scheme. (**B**, **C**) ChIP results demonstrate that the binding of pSTAT4 to 15-PGDH promoter is significantly increased by G9a knockdown in CCLP1 cells (B), which was further verified in SG231 cells (C). * $p < 0.01$ vs. corresponding control. (**D**) Representatives immunoblots show that G9a knockdown by shRNA did not influence pSTAT4 level in CCLP1 and SG231 cells. (**E**) STAT4 overexpression increases 15-PGDH protein level in CCLP1 and SG231 cells. (**F**) STAT4 and 15-PGDH expressions are positively correlated in CCA patients' tissues from dataset GSE76297.

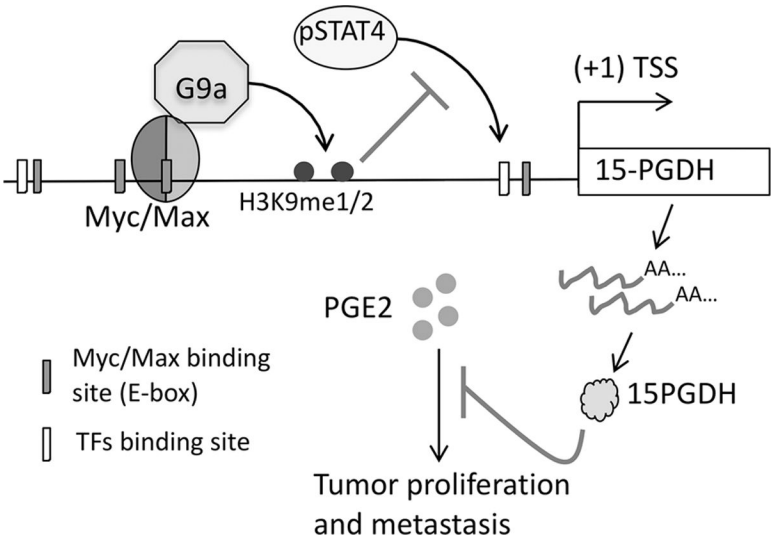

Figure 7. Schematic illustration of how G9a affects CCA development through regulating 15-PGDH.